Journal Pre-proof

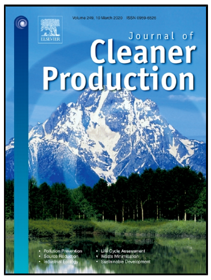

Mapping The Flood Risk to Socioeconomic Recovery Capacity through a Multicriteria Index

Osvaldo Moura Rezende, Anna Beatriz Ribeiro da Cruz de Franco., Antonio Krishnamurti Beleño de Oliveira, Francis Martins Miranda, Ana Caroline Pitzer Jacob, Matheus Martins de Sousa, Marcelo Gomes Miguez

PII:	S0959-6526(20)30298-5
DOI:	https://doi.org/10.1016/j.jclepro.2020.120251
Reference:	JCLP 120251
To appear in:	*Journal of Cleaner Production*
Received Date:	22 February 2019
Accepted Date:	23 January 2020

Please cite this article as: Osvaldo Moura Rezende, Anna Beatriz Ribeiro da Cruz de Franco., Antonio Krishnamurti Beleño de Oliveira, Francis Martins Miranda, Ana Caroline Pitzer Jacob, Matheus Martins de Sousa, Marcelo Gomes Miguez, Mapping The Flood Risk to Socioeconomic Recovery Capacity through a Multicriteria Index, *Journal of Cleaner Production* (2020), https://doi.org/10.1016/j.jclepro.2020.120251

Mapping The Flood Risk to Socioeconomic Recovery Capacity through a Multicriteria Index

Osvaldo Moura Rezende.[a,c*] e–mail: omrezende@coc.ufrj.br

Anna Beatriz Ribeiro da Cruz de Franco.[b] e–mail: annabfranco@poli.ufrj.br

Antonio Krishnamurti Beleño de Oliveira [b] e–mail: krishnamurti@poli.ufrj.br

Francis Martins Miranda [b] e–mail: francismmiranda@gmail.com

Ana Caroline Pitzer Jacob [c] e–mail: caroline@aquafluxus.com.br

Matheus Martins de Sousa [a] e–mail: matheus@poli.ufrj.br

Marcelo Gomes Miguez [a,b,d] e–mail: marcelomiguez@poli.ufrj.br

[a] Programa de Engenharia Ambiental – Escola Politécnica. Universidade Federal do Rio de Janeiro, Rio de Janeiro, Brasil

[b] Programa de Engenharia Civil – COPPE. Universidade Federal do Rio de Janeiro, Rio de Janeiro, Brasil

[c] Aquafluxus Water Resources Environmental Consulting, Rio de Janeiro, Brasil

[d] Programa de Engenharia Urbana – Escola Politécnica. Universidade Federal do Rio de Janeiro, Rio de Janeiro, Brasil

HIGHLIGHTS

- The usual risk assessment may disregard socioeconomically vulnerable communities;
- Measuring the Socioeconomic Recovery Capacity of urban areas prone to flooding;
- Multicriteria approach strengths social bias discussion into flood risk management;
- Flood mapping provides a spatialized view of the risk for different areas;
- Sustainability indicators to assess multi-scenarios can support decision- making.

* Corresponding author. Athos da Silveira Ramos Avenue, 149 - Block I – Room 206 – Cidade Universitária, Rio de Janeiro - RJ, 21941-909. Phone number: +55 21 3938-7830

MAPPING THE FLOOD RISK TO SOCIOECONOMIC RECOVERY CAPACITY THROUGH A MULTICRITERIA INDEX

ABSTRACT

Flood risk is generally composed of two parts: the probability of happening a hazardous event and its consequences. The first part is the source of risk and it is mainly given by the flooding magnitudes, although flow velocities and flooding permanence may play important roles. The second one reflects the vulnerability of the socioeconomic system exposed to flooding. Three aspects can represent vulnerability: *exposure*, *susceptibility* and *value*. Additionally, resilience can work to diminish vulnerability, incorporating the system responsive capacity. However, it is usual that risk assessment considers only the direct damage of flooding, tending to prioritize areas with high potential losses using an economic-based approach. This approach can exclude socioeconomically vulnerable communities from receiving proper attention and consequent investments in flooding mitigation measures. In this context, this paper presents an index to measure the Socioeconomic Recovery Capacity of urban areas prone to flooding through a multi-criteria approach, contributing to knowledge by introducing a social bias into flood risk discussion. The Flood Risk to Socioeconomic Recovery Capacity Index (Ri-SoRCI) considers the relative potential damage of flooding events, based on the capacity of the affected inhabitants to recover from losses. The Ri-SoRCI represents a socioeconomic parcel of the flood risk, through two indicators. The first represents the economic recovery capacity of an impacted region. The second indicates the region's social vulnerability. The Ri-SoRCI was applied to the Canal do Mangue basin, in Rio de Janeiro, Brazil, supported by an environmental modeling tool able to simulate flooding phenomena with an integrated approach. The result shows the risk variation for different areas, from the socioeconomic point of view, subsidizing decision-making for public investments and allowing the construction of sustainability indicators to assess multiple scenarios. The case study validated the proposed index.

KEYWORDS

Flood vulnerability; flood risk; flood risk management; flood mapping; mathematical modeling; urban stormwater planning.

1. INTRODUCTION

The urban population of the world has been growing rapidly over the last years, having increased from 30% in 1950 to 55% in 2018. By 2050, the world's population residing in urban areas is projected to be 68% (DESA/UN-WUP, 2018). The current number of people at risk from flooding is about 1.2 billion and, by 2050, this number rises to 1.6 billion, nearly 20% of the world's population (WWAP/UN-Water, 2018). Urbanization associated with changes in land cover results in significant increase of impervious areas and decrease in vegetated surfaces, heavily modifying the characteristics of the surface runoff (Goonetilleke *et al.*, 2005), increasing peak flows and stormwater volumes (Barbosa *et al.*, 2012). Such effects associated with a forecasted increase in the precipitation intensity, caused by global climate change (Meehl *et al.*, 2007), can intensify the stress on drainage infrastructures and increase flood hazards (Hoegh-Guldberg *et al.*, 2018), expanding flood prone areas (Petit-Boix *et al.*, 2017). The increased flood risk encountered in today's cities is mainly related to changes in land use and to the intense process of urbanization (Gogate *et al.*, 2017). Bradshaw *et al.* (2007) highlights that stopping deforestation can help to alleviate the incidence and the severity of flood events, which is, in fact, the opposite of what happens during the process of intense urbanization, usually leading to large changes in water flow patterns (De Roo *et al.*, 2003).

On the other side, when trying to measure flooding effects in their diversity, Multi-Criteria Analysis (MCA) can address multiple aspects of flood risk management, such as social-environmental issues, and support decision makers and stakeholders in the decision-making process (Jha *et al.*, 2012). Multiple scenarios simulation and mapping can also aid in the understanding of the problem dynamics. Balica *et al.* (2009) developed and applied an index built from a set of various indicators to quantify flood vulnerability and stated that the identification of flood prone areas based on the index could improve the decision-making process, guiding the prioritization of investments.

Considering this perception, the present paper proposes an index based on MCA to support the planning and design of urban drainage solutions, but in this new proposal the method surpasses the economic bias of computing only direct economic losses in the risk assessment. This index represents the socioeconomic parcel of the flood risk, being named as the Risk to Socioeconomic Recovery Capacity Index (Ri-SoRCI). The Ri-SoRCI is calculated through two indicators, the Relative Value Indicator (I_{RV}) and the Vulnerable People Indicator (*Ivp*), bringing light to the urgent necessity to correct the tendency of classical risk evaluation that tend to prioritize the richer areas of a city (where higher economic losses occur), in the flood risk management (FRM) process.

Within this strategy, the novelty of the proposed risk evaluation method is perceived in the establishment of a proper approach to introduce social aspects into the public investment decision-making process, including the poorer areas of the city in the discussion, concerning their relative capacity to self-recover from the damages suffered.

The Ri-SoRCI is applied to the Canal do Mangue basin, located in the central region of Rio de Janeiro, Brazil. This region is known for suffering historical severe impacts from floods, where a mix of formal and informal urban areas is settled.

The results show the vulnerabilities of different places of the basin, from a socioeconomic point of view. The flood risk mapping through Ri-SoRCI application can subsidize the decision-making process for investments in protection measures, also concerning the areas that are socially more vulnerable.

2. LITERATURE REVIEW

The traditional urban stormwater practices were usually focused on end-of-pipe measures (Rezende, 2018). However, simply adapting the network dimensions to the new drainage conditions becomes a problem over time, working by transferring floods to the already densely occupied urban environment. This context reinforces the necessity to introduce FRM in the decision-making process (Sayers *et al.*, 2013). According to The Flood Directive, published on the Official Journal of the European Union, flood risk management plans should address all aspects of an integrated flood risk management, including prevention, protection, preparedness and response phases, taking into account the specificity of each river basin or sub-basin as a socioeconomic (and vulnerable) system.(European Union, 2007). Kelman (2003) collected some different variations of risk definition and found that they were generally composed of two parts: the *possibility* of an event to occur and the *impact* associated with the occurrence of that event, as also stressed by Sayers *et al.* (2002). Therefore, in a simple formulation, the risk can be considered as equal to the hazard multiplied by the consequences that arise from the exposed system vulnerability (Tingsanchali, 2012). The flood risk has a peculiarity that distinguishes it from the classic risk definition, since the hazard, although related to the probability of occurrence of an intense rainfall, is materialized by the consequent flood resulting from the interaction between the rainfall and the basin. In this way, the hazard in flood risk management can be modified through structural measures that aim to control and mitigate floods (UNESCO, 2013).

The second part of risk composition reflects the vulnerability of the local population exposed to flood events and it is materialized by the consequences of flooding. It considers three aspects (Jha *et al.*, 2012): *exposure*, indicating the presence of assets and people in the affected area; *susceptibility,* representing the propensity of population and goods to suffer damages during the flood event; and *value*, which quantifies the potential monetary impacts. Over the last years, *resilience* was included to compose the risk evaluation, as we can see in several published works (Meerow et al., 2016). Gallopín, (2006) presented the resilience as the flip side of vulnerability, once it is related to the capacity of response of the vulnerability. Johannessen and Wamsler (2017) proposed an overview of the resilience in the urban water system, dividing it in three levels: (1) Socioeconomic operation in focus; (2) External hazard considerations are taken; (3) A larger social-ecological system. Liao (2012) particularized the term resilience to urban flooding, defining it as the capacity of a city to tolerate flooding events and to reorganize its urban system operations if physical damage and socioeconomic disruption occur. The concept of resilience arises opposing to the materialization of risk, by reducing vulnerability and consisting of the ability to absorb impacts and recover from unexpected events associated with natural disasters (Sayers *et al.*, 2013).

Therefore, flood risk management can act by reducing the vulnerability regarding human health, environment aspects, cultural heritage and economic activities (Vanneuville *et al.*, 2011) and/or increasing the resilience of the affected areas (Mendoza-Tinoco *et al.*, 2017). Understanding vulnerability is important to compose a broad framework where resilience also appears. In recent studies, this term has gained multidisciplinary characteristics, incorporating not only structural aspects but both human and social dynamics (Silva, 2017). When applied to the disaster risk reduction discussion, vulnerability responds to the socially constructed pattern of a community that makes it more susceptible to damages and losses (Lavell *et al.*, 2003). On the other side, the *lack of resilience* represents the political and community behavior, when not prepared to absorb a potential negative impact of a dangerous phenomenon and unable to return to an acceptable functioning state.

The flood risk concept adopted in the present study refers to the UNESCO definition as observed in Figure 1 (UNESCO, 2013).

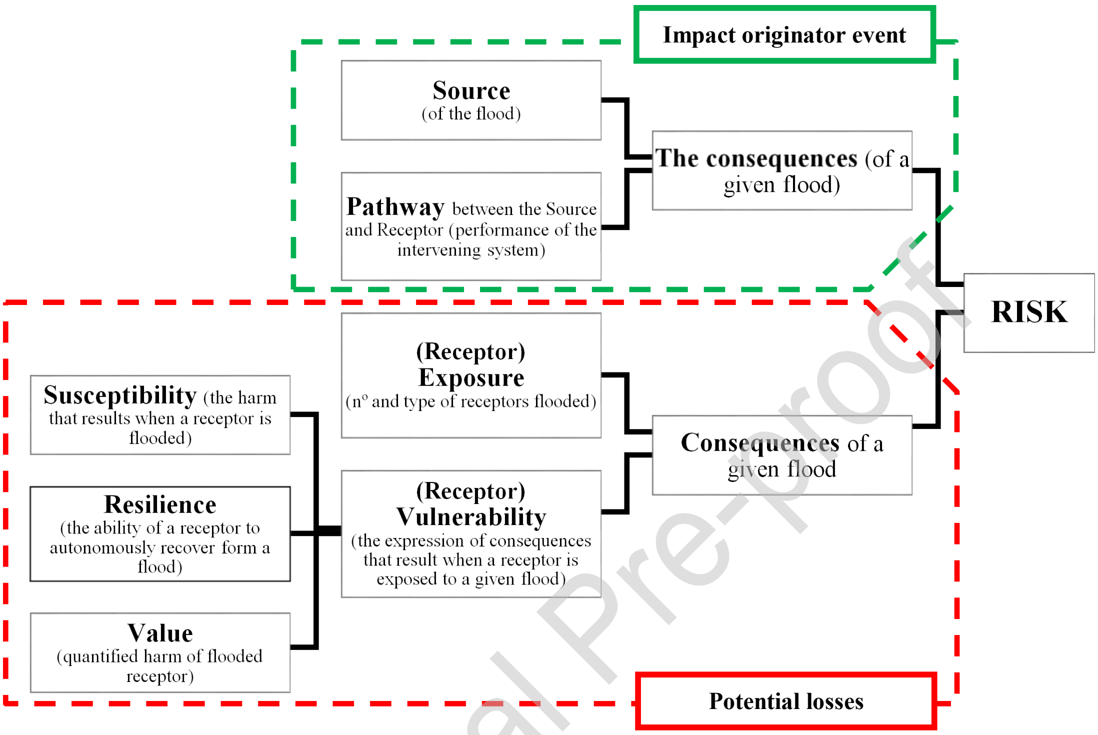

Figure 1. The components of risk (adapted from UNESCO, 2013)**.**

When focusing on social aspects, the vulnerability approach tends to be directly related with the resilience discussion, also considering responsiveness, recovery capability and adaptation aspects. In a flood management discussion, reducing social vulnerability is often neglected (Saito, 2014), being prioritized the adoption of structural measures to increase the resistance of the system (Nur and Shrestha, 2017) and reduce economic losses. A flood resilient approach in urban environments, in practice, involves multiple interventions at different spatial and temporal levels, and the implementation of a decentralized, bottom-up, flexible management structure and stakeholder commitment (Zevenbergen *et al.*, 2008). To cover this demand, Multi-Criteria Analysis tools (MCA) are largely used, providing a structured way for comparing benefits and costs that are often expressed in different units (Wouter Botzen *et al.*, 2019), not necessarily in monetary terms. However, the application of MCA for flood risk assessment in spatial approaches is a relatively new concept (Shivaprasad Sharma *et al.*, 2018), which has been widely used in recent years due to its easy application and great capability of handling scarcity of data (Xiao *et al.*, 2018). It is also an easy way to communicate results.

Mahmoud and Gan (2018) have proposed a method to measure the flood susceptibility, considering only physical aspects of the territory, providing a rapidly applying tool to classify areas accordingly to their prone to flooding. However, socioeconomic susceptibility should also be considered to guarantee social equality. Aiming at defining the benefit-cost analysis of using green infrastructures to control stormwaters, Nordman *et al.* (2018) considered the benefits of avoided stormwater runoff costs, pollution reduction, and landscape aesthetic enhancement, in order to compare several design alternatives at a given place. However, the lack of avoided social impacts in the benefits makes the method unfeasible to hierarchize flood control alternatives in poorer regions where costs may be low, pollution may be greatly dependent on the lack of sewer systems and landscape degradation is already in place.

Zeleňáková *et al.* (2019) applied the flood risk mapping to propose effective flood protection in a case study, considering the expected damage of a given flooding event. The authors sustained that flood protection structures should cost less than the estimated damage (which is usually the case), but left out the social impacts, which could induce the decision of prioritizing richer areas, where the most valuable assets are exposed.

In a more comprehensive study, Chuah *et al.* (2018) have highlighted the role of social-fairness in decision-making of flood control public investments. However, the FRM approach defined in their study is still strongly based on a direct cost-benefit analysis. In the own words of these authors (*ibid.*) this approach was adopted with the objective of maximizing the financial efficiency of FRM practices. Shivaprasad Sharma *et al.* (2018) have applied the MCA to classify risk zones, considering a multi-layer vulnerability approach. The proposed vulnerability indicators have addressed socioeconomic, infrastructure and land use aspects. The socioeconomic layer used data of household composition, gender (female), poverty and unemployment (illiterate population). However, although considering social aspects, the relative material losses and the recovery capacity were not addressed.

The state of art in flood risk management converges to understand the adaptive capacity as the best strategy to achieve more resilient and sustainable cities. Therefore, the evaluation of socioeconomic vulnerability concerning the recovery capacity of inhabitants can be a useful way to define better strategies to mitigate flood impacts in social environments.

3. MATERIAL AND METHODS

The Risk to Socioeconomic Recovery Capacity Index (Ri-SoRCI) represents the socioeconomic portion of flood risk, by multiplying a relative value indicator (I_{RV}) and a social vulnerability indicator (I_{SV}), with their related weights

The composition of Ri-SoRCI is presented on Figure 2 and it formulation is given by Equation (1).

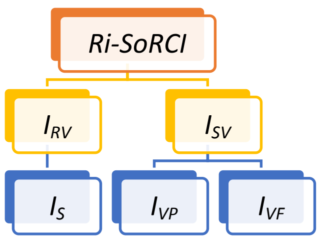

Figure 2. Composition of Risk to Socioeconomic Recovery Capacity Index (Ri-SoRCI)

$$Ri\_SoRCI = (I_{RV} \cdot a) + (I_{SV} \cdot b) \tag{1}$$

The parameters *a* and *b* are the weights associated with each sub-index. At this stage of the research, the weights assume equal values, since the main aim of this study is to propose the new index formulation. Defining the relative importance of each term in the risk composition is an important step of the process, but it should be done after validating the proposed method. Besides that, the process to define this relative importance is something that may vary from case to case, and which should be a prerogative of decision makers.

The relative value indicator (I_{RV}) relates flood height with the potential damage of flooding, according to the income of the population directly exposed to floods. The damages are related to the susceptibility of buildings in suffering flood losses, represented by the building susceptibility indicator (I_S). Therefore, the index allows the internalization of the hazard.

This index also considers the physical vulnerability of people that can suffer more in situations of hazard, represented by the portion of the population aged more than 60 and less than 15. The hazard indicator, in this case, is represented by the velocity factor (I_{VF}).The social vulnerability index proposed by the University of Amsterdam (Koks *et al.*, 2015) considers a similar age group to represent the most vulnerable population. Hence, I_{VF} specifies the potential impact of water flow on human stability, according to the product of flow velocity by flood depth (Reiter, 2000). This relation gives the social vulnerability indicator (I_{SV}).

The next sections present each indicator's composition.

3.1. Relative value indicator – I_{RV}

The I_{RV} represents the economic recovery capacity of a region after the occurrence of a flood event. It is calculated by the relation between potential economic losses and the capacity to replace these losses, which may be calculated by the difference between the total income and the average expenditure of a family during a year. This difference is estimated according to the Brazilian Household Budgets Survey, depending on the income range (IBGE, 2004) and it represents the savings capacity of a family. In this way, the I_{RV} intends to represent a relative importance value, instead of using the direct relation with monetary losses.

Differently from the most recent studies in the same line of research, as discussed earlier in the literature review section, the strategy of adopting the relative value to measure socioeconomic impact allows evaluating not an absolute loss, but the ability to recover from the damage suffered. The formulation of the I_{RV} indicator is given by Equation (2).

$$I_{RV} = \frac{(CDB + CDC) \cdot A_B \cdot I_S}{(12 \cdot TI \cdot RC)} \quad \overset{if}{\Rightarrow} RC > 0{,}0 \ (income \geq \text{US\$810})$$
$$I_{RV} = 1 \quad \overset{if}{\Rightarrow} RC = 0{,}0 \ (income < \text{US\$810}) \tag{2}$$

The numerator in I_{RV} equation is the potential damage to buildings and their contents in a region. The denominator represents the recovery capacity of the population exposed in that region, given by the product of the total annualized income (12 · TI) by the relationship between income and average expenditure, which represents the average replacement capacity (RC). The RC calculation considers the difference between the average income and expenditure of each analysis unit divided by the total income of that unit, indicating the amount that can be used to recover from unpredicted damages. The values of RC are defined according to the Brazilian Household Budgets Survey, depending on the income range (IBGE, 2004), as presented in Table 1.

Table 1. Average capacity of RC replacement, related to income range

Income range	RC
Under US$810.00	0.0000
From US$810.00 to US$1,081.00	0.0420
From US$1081.00 to US$1,622.00	0.0768
Above US$1,622.00	0.1996

The damage costs to a building and to building contents (*CDB* and *CDC*) are calculated by equations (3) and (5), considering the Basic Unit Cost (*BUC*) and the percentage of damages applied to building and its contents (*PDB* and *PDC*). The estimation of these costs considers an average depreciation of the existing buildings, and the current formulation adopts the average value of 0.50. This simplification allows the application of the method in regions with lack of more precise data about the average age of the building stock, reducing field survey demands in an acceptable way. However, a desirable improvement in this approach could consider the real age of the buildings in the estimation of the flood economic losses, to contemplate depreciation costs as a time function.

Equations (4) and (6), describe the percentages of damaged buildings and contents, respectively PDB and PDC, and they were based on previous studies of Salgado (1995). The equations represent the *flood height vs. damage* function, estimated for different economic patterns of residential buildings. They were originally formulated to calculate the total damage of flooding for incremental increases of 25 cm in water depths. For each flood height, the components or structures of the building subject to damage were identified, the monetary value of the damage, considering the basic unit costs (BUC), was estimated and, finally, the damage associated with the water level was calculated. The damage values are calculated as a percentage of damaged structure and/or contents, depending on water depths, multiplied by the total value of building structure and/or contents. In Brazil, the *BUC* is given by the Brazilian Chamber of Construction Industry (CBIC, 2019, in Portuguese). Therefore, the estimation of *CDB* and *CDC* assumes a local interpretation, depending on socioeconomic aspects of the considered study area.

Similar studies can be found in technical literature. Dutta *et al.*, (2003) calculate the economic loss using a mathematical hydrologic model, considering different land-use features, to obtain simulated flooding parameters. Machado *et al.* (2005) developed standardization flood depth-damage curves, allowing the estimation of damages of a given inundated area. Penning-Rowsell and Chaterton (1980) created a methodology to simplify the assessing to economic benefits of flood alleviation and land drainage schemes.

The Building Susceptibility Indicator (I_S), given by equation (7), indirectly considers the average number of floors in a given area. Therefore, the lower the average height of the buildings, more susceptible to flood the constructed area is. The I_S is independent of storm events and drainage network conditions. Information on the height of the buildings in the Canal do Mangue basin was obtained from the Municipal Institute of Urbanization Pereira Passos (IPP, 2019).

Next, the variables that compose Equation (2) are presented.

$CDB = [(0.5 \cdot BUC_E) \cdot PDB]$ → Cost of damage to building (3)

BUC_E → Basic unit cost of building structure, according to the economy class

$PDB = 0.0811 \cdot \ln(h) + 0.1338$ → Percentage of damage on building structure as a function of water depth h (4)

$CDC = [(0.5 \cdot BUC_C) \cdot PCD]$ → Cost of damage to building contents (5)

BUC_C → Basic unit cost of contents, according to the economy class

$PDC = 0.3878 \cdot \ln(h) + 0.3788$ → Percentage of damaged contents as a function of water depth h (6)

A_B → Total constructed area in the region under analysis

$I_S = {\sum_{i=1}^{n} I_A}/{n}$ → Indicator of building susceptibility, represented by the average height of buildings in the region under analysis (7)

I_A → Height indicator of building i, given in accordance to Table 2

n → Number of buildings

TI → Total Income of the analyzed region

RC → Average recovery capacity of the analyzed region, according to Table 1

The Building Height Indicator (I_A) represents the average height of buildings in the analyzed unit. Its normalization is done by assuming that one-floor buildings are more prone to suffer relative damages from flooding, since all the built areas are in the same level of the flooding. The I_A represents a relative potential damage, showing that one floor buildings are more exposed to flooding waters than multi-floors buildings. Therefore, buildings with less than 5.0 meters (assumed as the limit to build a second floor) receive the highest indicator, equal to 1.0, representing dwellings and buildings with only one floor. Then, the indicator values vary every 2.5 meters, indicating a new floor to each one, as it can be seen in Table 2. Figure 3 shows the limits of the buildings' heights used to normalize the indicator, with values varying from 0 to 1.

Table 2. Values of Height Indicator (I_A), related to the height of building (H).

Height of building H	Height Indicator I_A
H < 5.0m	1.00
5.0m < H < 7.5m	0.50
7.5m < H < 10.0m	0.33
10.0m < H < 12.5m	0.25
H > 12.5m	0.10

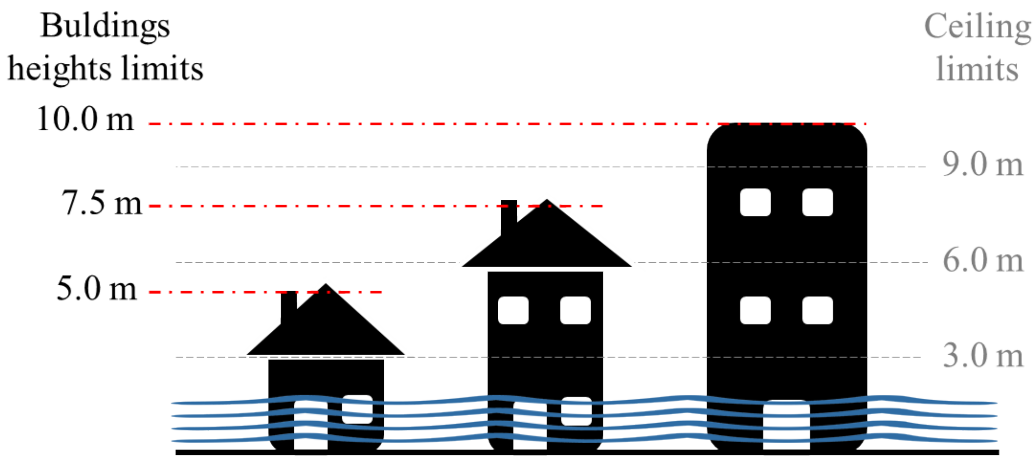

Figure 3. Limits of buildings' heights used to the Height Indicator (I_A) normalization

3.2. Social vulnerability indicator – I_{SV}

The I_{SV} represents part of the social vulnerability of a region, related to the people potentially vulnerable to flood events, from a physical point of view. The I_{VP} considers two parcels, one taking the direct proportion of the more vulnerable population, the one that is less than 15 years and more than 60 years old; and the other takes the percentage of the non-vulnerable population. Therefore, it is considered the entire affected population.

Each parcel is differently affected by the *velocity factor* (I_{VF}) because it directly indicates the potential impact of water flow on human stability during a flood event (Lind *et al.*, 2004).

The general formulation of I_{SV} is given by Equation (8).

$$I_{SV} = a \cdot \left[(I_{VP})^{n1} \cdot (I_{VFv})^{n2} \right] + b \cdot \left[(I_{NP})^{n3} \cdot (I_{VFn})^{n4} \right] \tag{8}$$

In Equation (8), a, b, $n1$, $n2$, $n3$ and $n4$ represent weights related to sub indicators of exposed people and co-related hazard thresholds, that are represented by proper velocity factors. In the present stage of the research, the weighting process considered equal values for all the indicators. Although recognizing that this is an important task, the main goal here is to test the method and defining the weights to reach a more representative value is not a current key point, as already mentioned in the previous discussion. These sub-indicators are calculated by using Equations (9), (10), (11) and (12).

$$I_{VP} = \frac{N_{VP}}{P} \rightarrow \text{indicator of more vulnerable persons} \tag{9}$$

$$I_{NP} = 1 - I_{VP} \rightarrow \text{indicator of non-vulnerable persons} \tag{10}$$

N_{VP} → Number of more vulnerable persons (aged under 15 and above 60)

P → Total population in the analyzed region

$$I_{VFv} = 0.9743 \cdot \ln{(VF)} + 2.3308 \rightarrow \text{Velocity factor indicator for vulnerable people (Figure 5)} \tag{11}$$

$$I_{VFn} = 1.0554 \cdot \ln{(VF)} + 1.3596 \rightarrow \text{Velocity factor indicator for non-vulnerable people (Figure 5)} \tag{12}$$

$$VF = V \cdot H \rightarrow \text{Velocity factor, given by the product between flow velocity } V \text{ and flood height } H \tag{13}$$

The normalization of I_{VF} considered previous studies on the stability of people exposed to water flows (Reiter, 2000), as shown in the graph of Figure 4. From this graph, two classifications were developed for stability loss of vulnerable and non-vulnerable groups, according to VF values (Table 3), which were normalized by a log function (Figure 5). This normalization of I_{VFv} and I_{VFn}, is defined by equations (11) and (12).

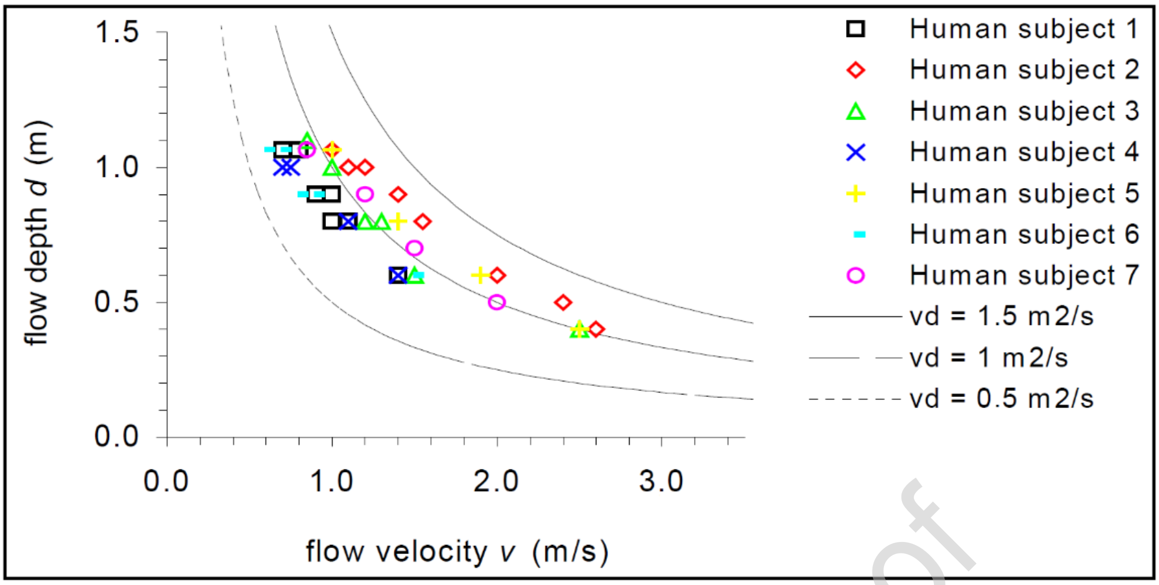

Figure 4. Loss of stability - Test results (Reiter, 2000).

Table 3. Classification of I_{SF} according to drag risk classes, related to the velocity factor VF.

Vulnerable persons			Non-vulnerable persons		
RISK	VF	I_{VFv}	**RISK**	VF	I_{VFn}
minimal	0.050	0.000	minimal	0.000	0.000
low	0.100	0.090	low	0.300	0.090
medium	0.175	0.630	medium	0.500	0.630
high	0.250	1.000	high	0.700	1.000

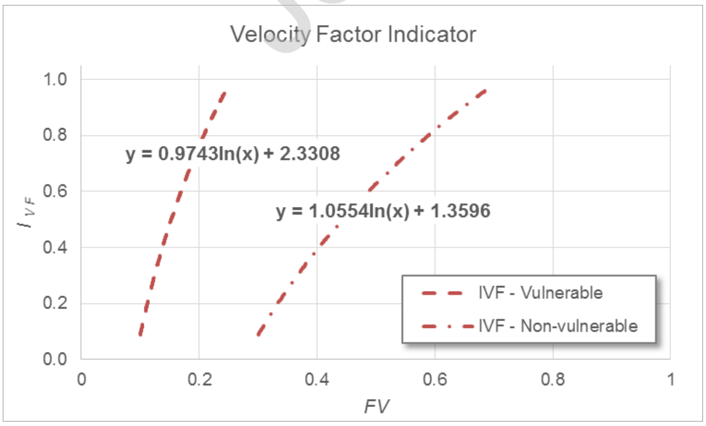

Figure 5. Normalization of I_{VF} according to the velocity factor VF

The Indicator of Vulnerable People (I_{VP}) depends only on the age composition of the population in a region. This information, in the case of this work, comes from the 2010 Demographic Census database (IBGE, 2010), which is the last available census in Brazil. As both indicators do not depend on flooding characteristics, they can be classified as independent indicators (Rezende *et al.*, 2018).

4. CASE STUDY

The proposed method is applied to a highly urbanized basin located in the Rio de Janeiro City central area. To asses flooding behavior and apply the index, a hydrologic-hydrodynamic model was built to simulate floods in the basin. The following sections present the study area and the flood modeling tool characteristics.

4.1. Study area

The *Canal do Mangue* basin (BCM) is located in the central region of the municipality of Rio de Janeiro, discharging at Guanabara Bay. The map of Figure 6 shows the BCM location. It has a drainage area of 45.4 km². The main watercourses of the *Canal do Mangue* basin are the Maracanã, Joana, Trapicheiros, Comprido and Papa-Couve rivers. These rivers have their headwater in the Tijuca Massif or in the Engenho Novo Range.

This watershed has suffered an enormous anthropic modification, both in land use and natural drainage system. The changes aimed at creating areas of landfills to allow the expansion of urbanization of the City of Rio de Janeiro over marshlands and even gaining some area from the Guanabara Bay.

This watershed is highly urbanized, mainly in the lower areas, with an urbanization rate of 81%. Figure 7 shows this situation. The remnants of Atlantic forest, found on the hills, are located in regions of high slopes, favoring a very rapid runoff, with little capacity of retaining rainwaters precipitated in intense hydrological events.

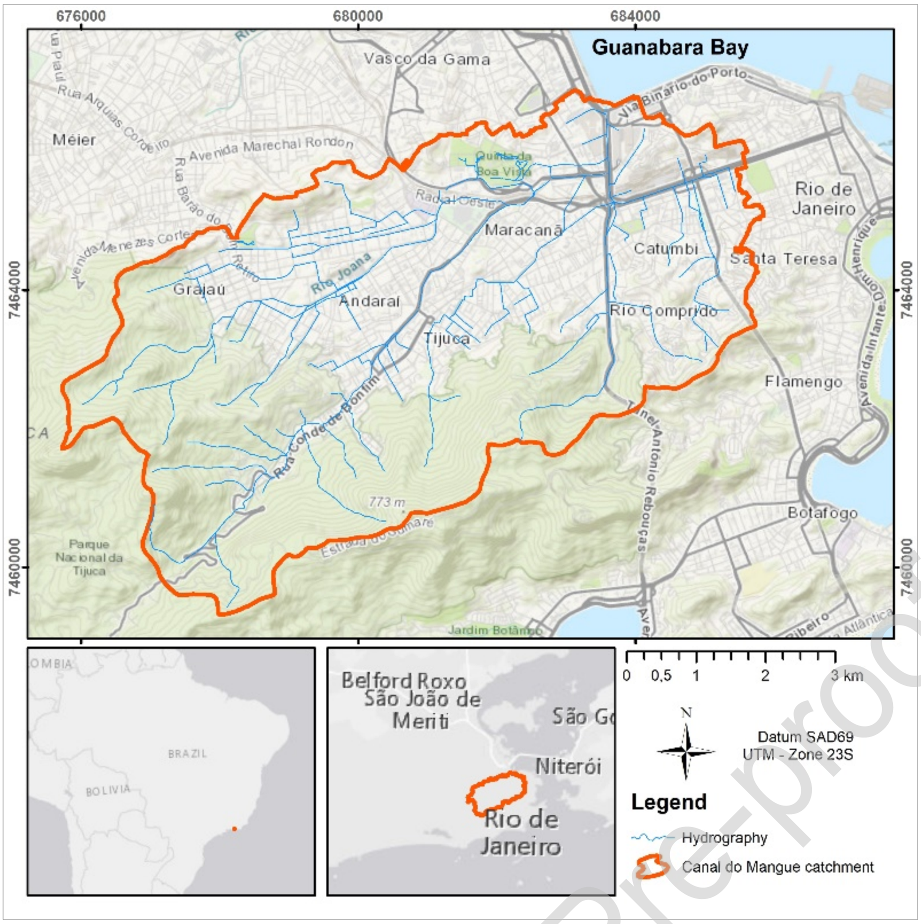

Figure 6. Location map of Canal do Mangue basin (Rezende, 2018).

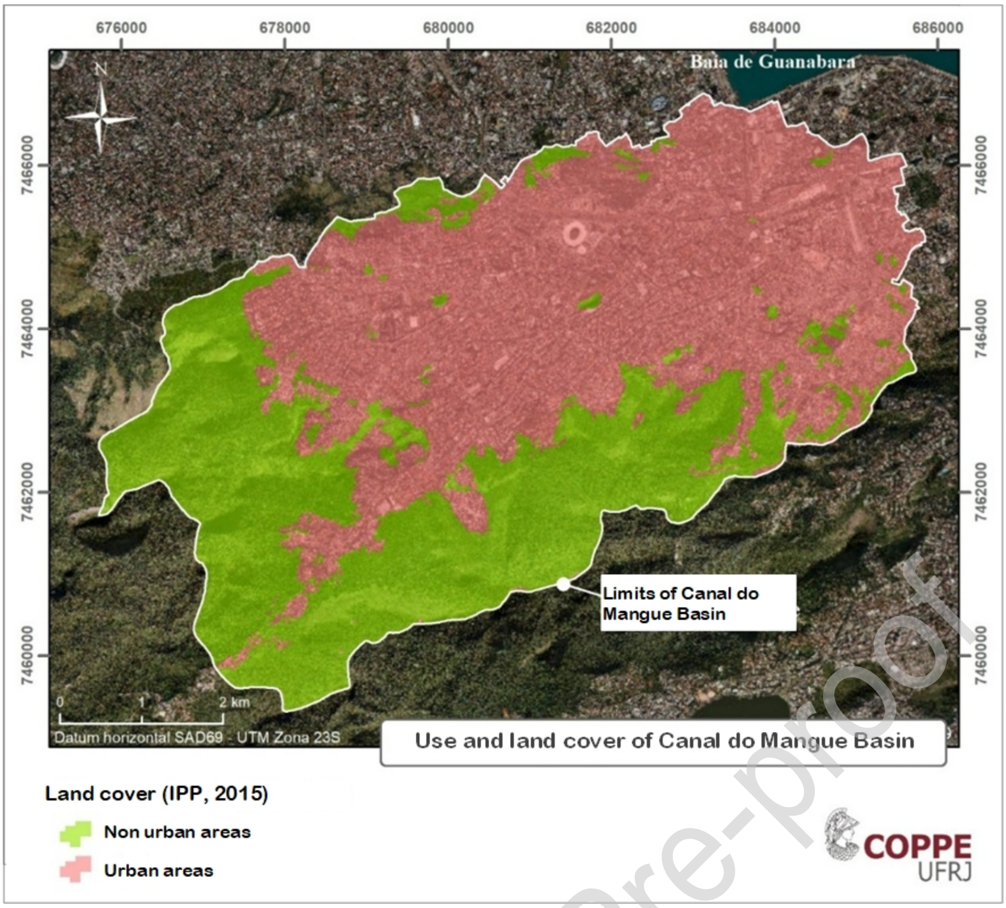

Figure 7. Urbanization of Canal do Mangue basin (Rezende, 2018).

In this context, the Canal do Mangue basin has almost no space for zoning changes, making it almost impossible to remove people and properties from flood risk areas. In this kind of situation, flood control actions must be grounded in urban drainage compensatory techniques. Therefore, the choice for the BCM as a case study had the following main motivations:

- Geographic importance: it is located between the central and northern zone of the city of Rio de Janeiro, and its territory is densely occupied and highly modified by the process of urban occupation;
- Historical importance: the basin shelters an old and consolidated occupation, including important reference points (like the Imperial Museum and the Maracanã Stadium), presenting serious flooding problems throughout the entire history of its occupation, being the subject of several previous studies and projects for flood mitigation;

- Economic importance: relevant roadways to the whole city are set in the region, with high potential to produce large traffic jams during heavy rains due to mobility interruption; besides that, the existence of different patterns of occupation, varying from slums to high standard neighborhoods offers a wide range of observation.

4.2. Flood modeling

The choice of MODCEL to perform the hydrological-hydrodynamic simulations in the *Canal do Mangue* basin was made based on its capacity to represent the entire watershed working together, as an interrelated system.

This model is based on the original work concept of Zanobetti and Lorgeré (1968) and assumes that the watershed can be subdivided in various types of flow-cells, which interact with each other through 1D flow equations. Additionally, a dual drainage approach supports this model: surface flow, open channels and storm sewers can be linked, so the flow can occur simultaneously on both layers – surface and underground (Silva *et al.*, 2017). More detailed description of MODCEL can be found in several published papers, since the first international publication in 2002 (Mascarenhas and Miguez, 2002) with its last version presented in Miguez *et al.*, 2017).

The *Canal do Mangue* watershed modeling base resulted 1,036 cells, containing 100 cells representing rivers and channels, 204 cells of storm drains, 681 urbanized plain cells and 51 slope cells, as shown in Figure 8.

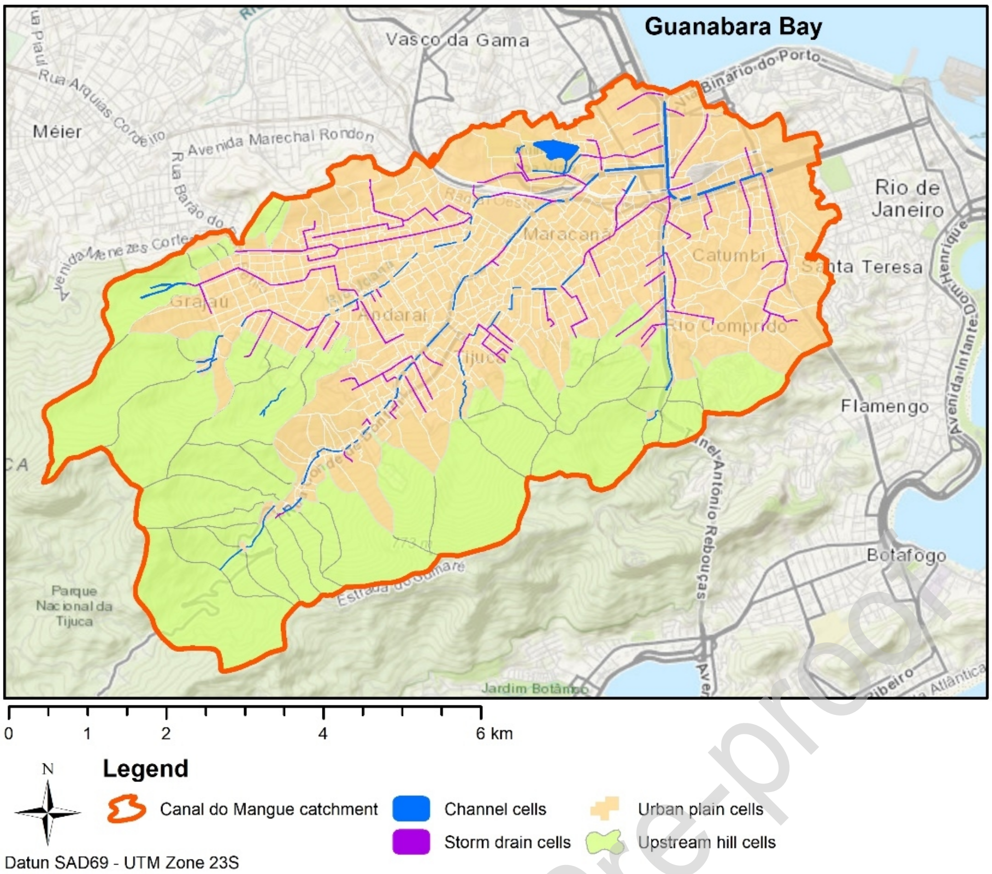

Figure 8. Division of Canal do Mangue basin in flow cells.

Calibration and validation.

The model was calibrated and validated for data measured in two 24h events, available at five rain gauges of Rio de Janeiro City Hall Alert System (Rio Alert), with data gathered at every 15 minutes, plus two stations installed within the Stormwater Master Plan of the Canal do Mangue basin (COPPETEC, 2000). The total rainfall measured in each event can be seen in Table 4.

Table 4. Total rainfall in millimeters measured in 24 hours on the events selected for calibration and validation of the mathematical model.

Station	PGRJ	PSTR	PSAD	PTJC	PABV	PDCV	PANDA
Calibration	127.4	66.9	103.1	92.3	101.5	88.9	113.6
Validation	66.78	13.89	35.62	35.42	15.79	29.5	50.05

The spatialization of the measured rainfall in the Canal do Mangue basin was made using the Thiessen Polygons Method. Both events were simulated and the water level results were compared with the measured data of fluvial stations installed during the elaboration of the Stormwater Master Plan of the Canal Mangue basin. The extension of the observed flooded areas was also considered in the calibration process.

The main calibration parameters in this modeling system are the runoff and Manning coefficients, as well as other hydraulic parameters associated with classical equations used in the hydraulic links of MODCEL, such as orifices and broad crested weirs. The runoff coefficient was defined according to land use and land cover of the basin, distinguishing between urban and non-urban areas. For the Manning coefficients used in the links between channel and storm drains cells (represented by Saint Venant dynamic equation), the method proposed by Chow was applied (1959). The values were defined according to the conditions presented in each stretch under analysis, identifying bed irregularities, abrupt transitions in the flow cross-section, and the occurrence of meanders or vegetation in the main channel.

Figure 9 shows the localization of rain gauges and fluvial gauges, as well as the results of the calibration process. The measured water levels in Maracanã River seems to show a data acquisition error. The point that makes the simulated results appear overestimated is not coherent with the expected hydraulic response in this river stretch. The water level behaviour should be similar to the Joana River responses, since both stations are located at an equivalent place in each sub-basin, draining similar areas. Therefore, it is expected that water levels in Maracanã River, at this point, reach 3.0 meters in water depth, what corroborate simulated results. Moreover, the doubtful value coincidently equals the average between the previous and following measured values, suggesting that this doubtful value was not really measured.

The validation results are shown in Figure 10. This whole process is described in detail in Rezende (2018).

Hydrological scenario.

The simulation scenario uses a rainfall event with 25 years of return period (RP). This RP was adopted due to the official Brazilian government requirement for flood control design, also agreeing with the technical instructions of Rio-Águas (Rio-Águas, 2010), the Municipal Foundation that responds for the urban waters management in Rio de Janeiro. The design rainfall is 180 minutes long (equivalent to the time of concentration of the basin), distributed temporally according to the alternate-block method (Chow et al., 1988; US Department of the Interior, 1987), as shown in Table 5. The total design rainfall shows how critical are the storms in Rio de Janeiro region, with the maximum rainfall intensity reaching 121.74mm/h.

Table 5. Design storm of proposed hydrological event.

T (min)	30	60	90	120	150	180	**TOTAL**
Rainfall (mm)	4.59	7.50	10.90	60.87	19.28	5.69	**108.84**

The simulation of the validation event resulted in maximum water levels very similar to the measured values, as showed in Figure 10.

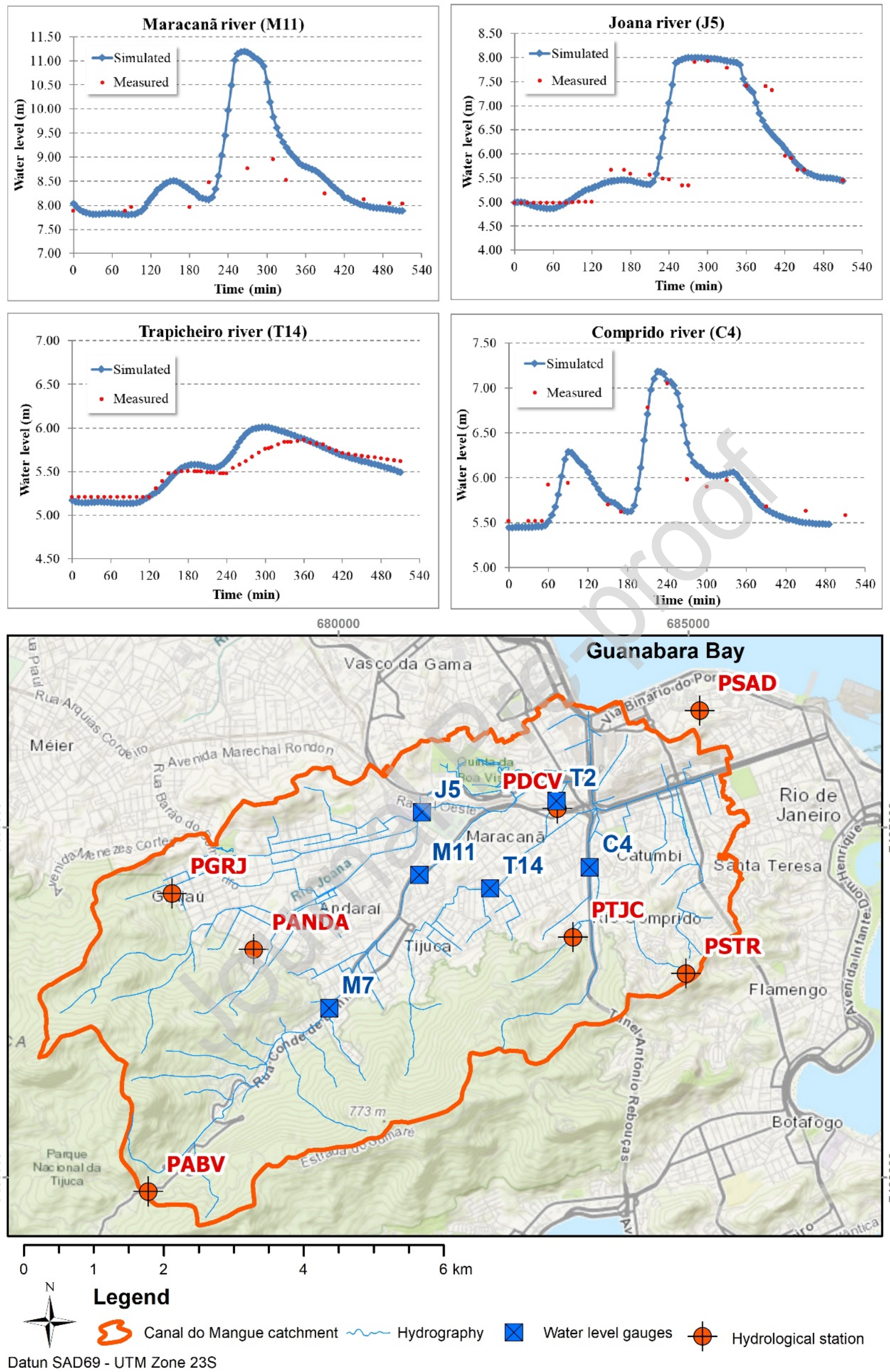

Figure 9. Localization of measuring stations and water level results of calibration process.

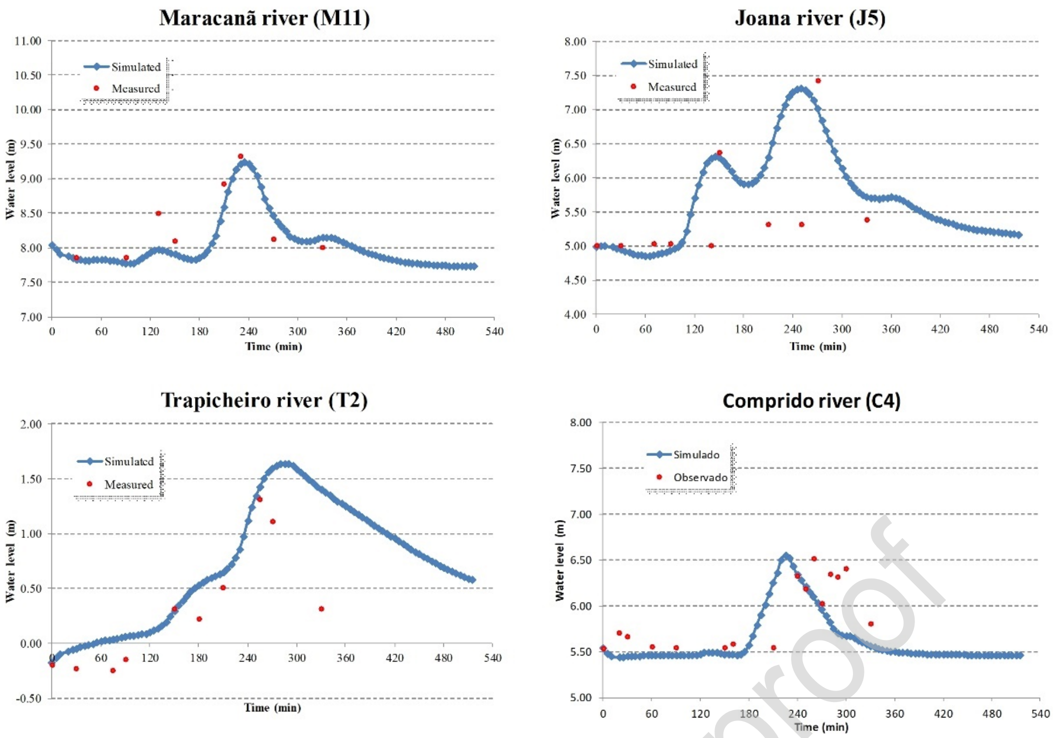

Figure 10. Water level results of validation process (see Figure 9 for localization of measuring stations).

5. RESULTS AND DISCUSSION

In order to relativize the risk based on a socioeconomic criterion, the Risk to Socioeconomic Recovery Capacity Index (Ri-SoRCI) corrects a tendency of the traditional risk assessment to prioritize areas occupied by higher income classes.

The susceptibility of buildings mapped for Canal do Mangue basin shows that the region presents a very high vertical occupation, characterizing a high-density urbanization. This urban configuration reduces potential relative damages on buildings, but exposes more people. The index seeks to represent the potential flood damage to the economic recovery capacity of local inhabitants, adequately representing and reducing the susceptibility to damage with the construction height. The spatialization of the I_S indicator in the Canal do Mangue basin is presented in the map of Figure 11.

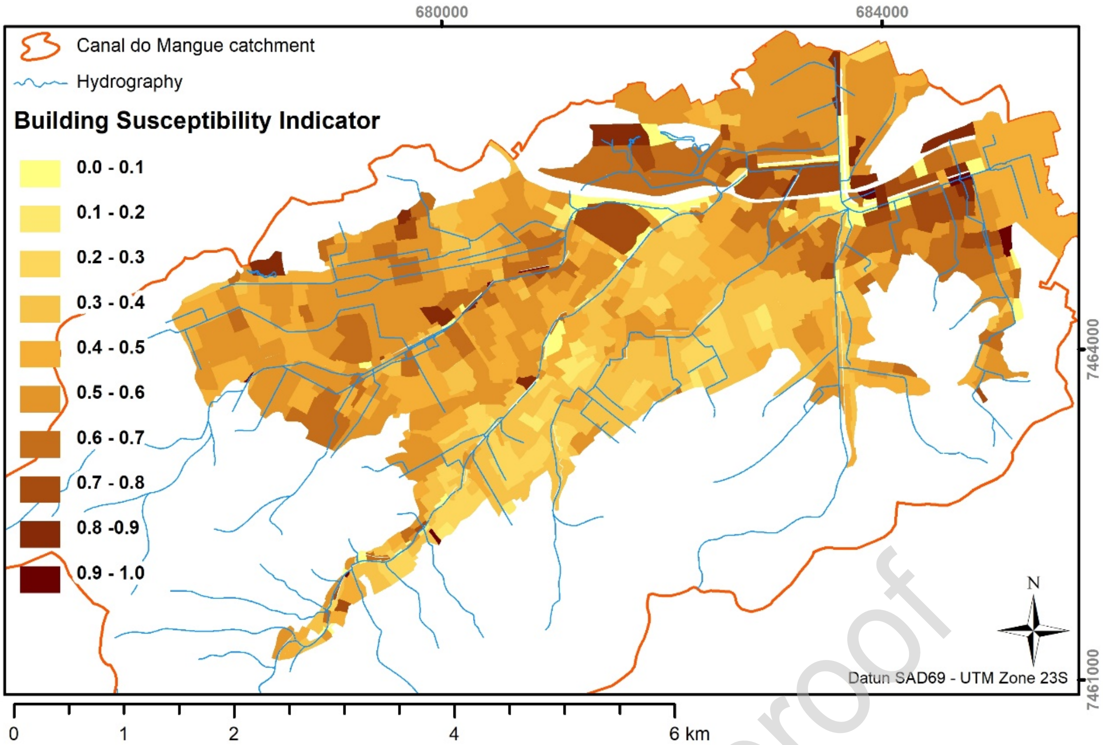

Figure 11. Mapping of building susceptibility indicators (I_S).

The income distribution of the interest area presents a reasonable variation on socioeconomic range, but with most of the basin showing a middle class occupation, according to Brazilian government classification. This distribution is shown in Figure 12.

The Relative Value Indicator uses the water level in a *depth-damage* curve, considering also the economic recovery capacity of the inhabitants. Thus, regions where people are poorer tend to present higher values of I_{RV}, given a flood depth. The water depths result of flood modeling, considering the 25 years design storm, is shown in Figure 13, allowing the observation of the areas that are most prone to flooding. These areas are concentrated along river paths and on plain regions of the basin. The Relative Value Indicator mapped for Canal do Mangue basin is presented in Figure 14.

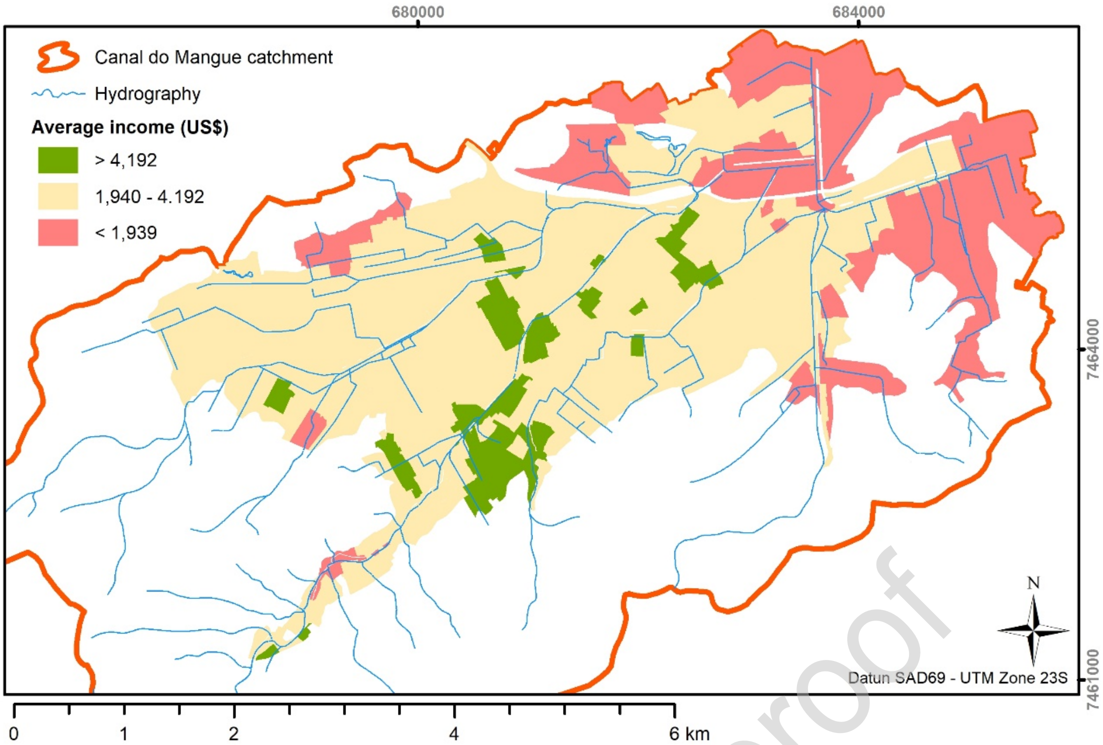

Figure 12. Socioeconomic mapping in the interest area of Canal do Mangue basin (Average mensal income in dollars – converted from Brazilian Real based on 2012 exchange values).

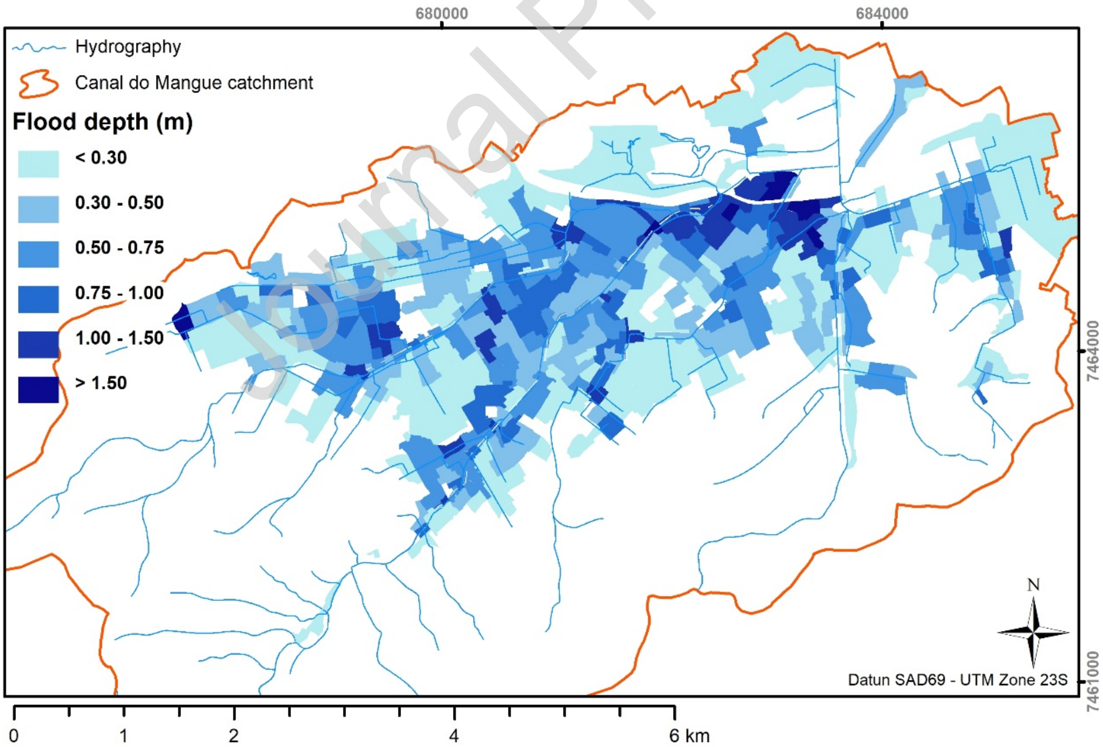

Figure 13. Flood mapping for a 25 years storm event in Canal do Mangue basin.

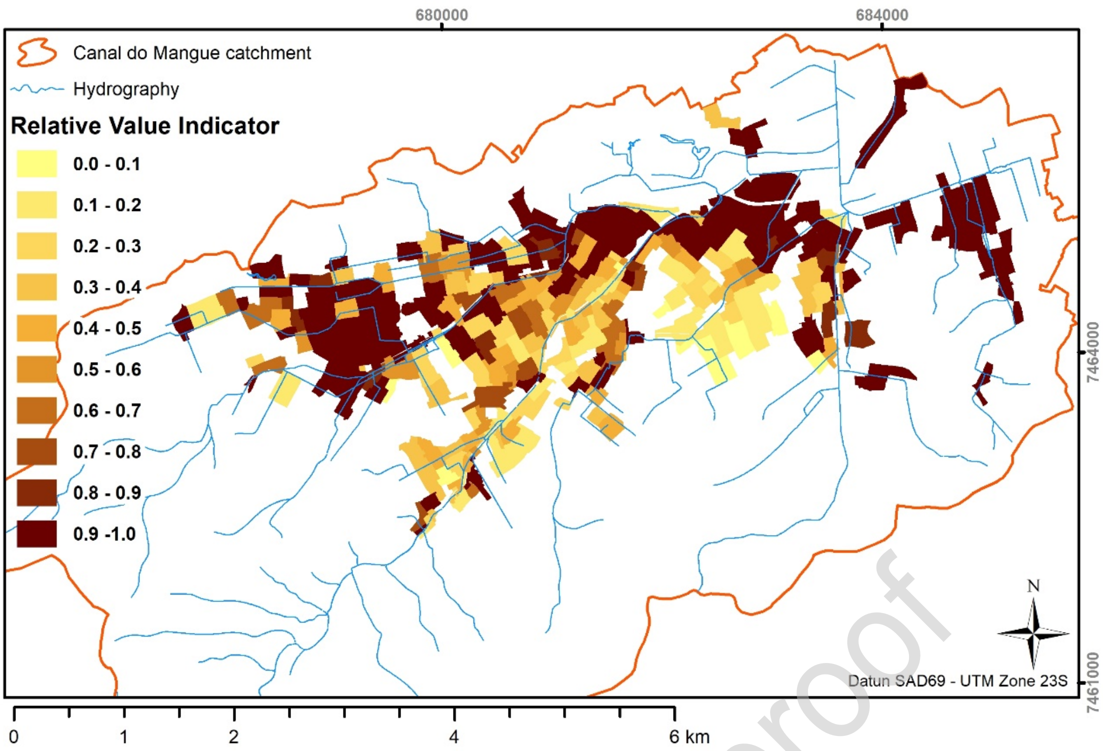

Figure 14. Mapping of the Relative Value Indicator (I_{RV})

For the estimation of social vulnerability, based on people's propensity to suffer damages during a flood event, the portion of the hazard relative to the Velocity Factor (I_{VF}), which influences the dragging capacity of the flow, is considered. The I_{VF} of vulnerable and non-vulnerable people, resulting from the simulated event, can be seen in the map of Figure 15. Some places present a water depth and/or flow velocity so high that even for non-vulnerable people (a), I_{VF} shows elevated values. The same flooding characteristics (water depth and flow velocity) results in a more critical profile for the vulnerable people (b), resulting in a darker map.

Figure 16 presents the mapping of I_{VP} in the Canal do Mangue basin, allowing one to conclude that population is affected in a relatively homogeneous way.

The results of the Social Vulnerability Indicator (I_{SV}) mapping can be seen in Figure 17.

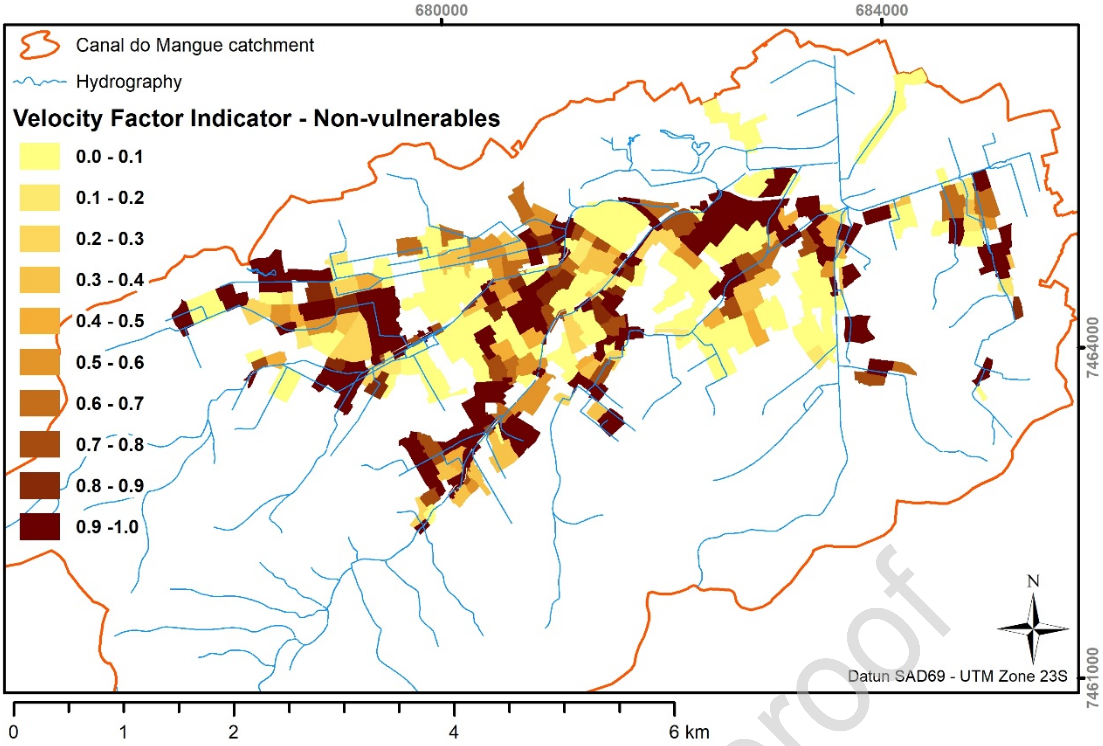

(a)

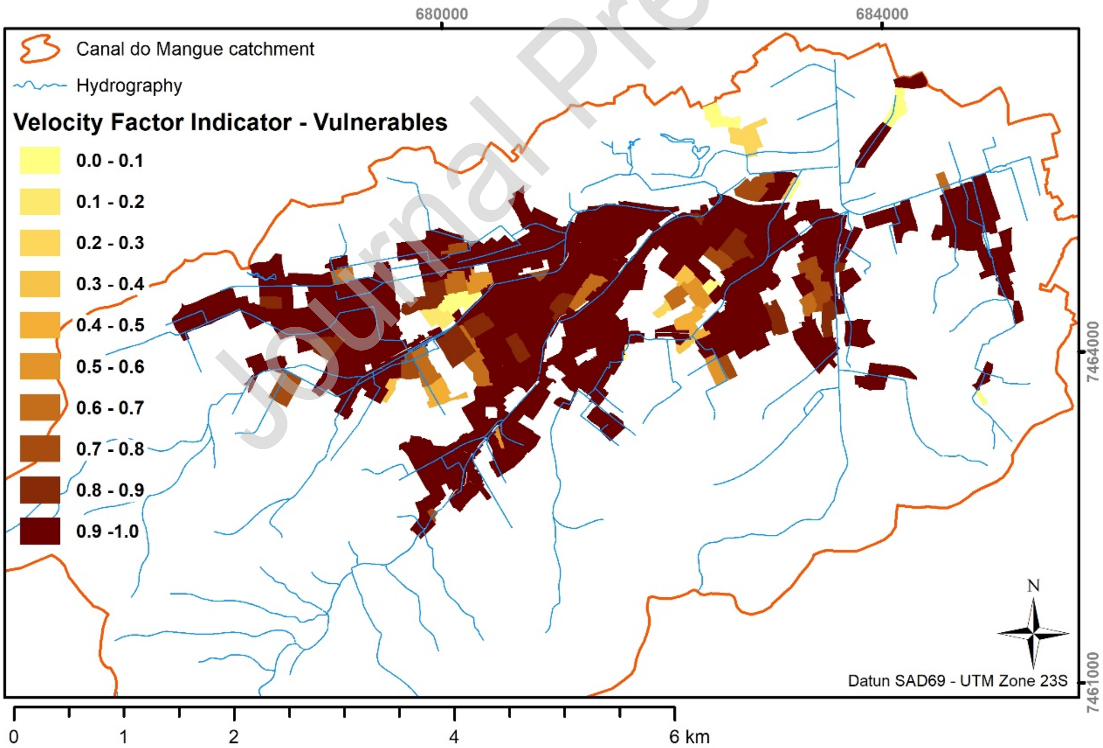

(b)

Figure 15. Mapping of the Velocity Factor Indicator (I_{VF}) considering (a) non-vulnerable and (b) vulnerable people.

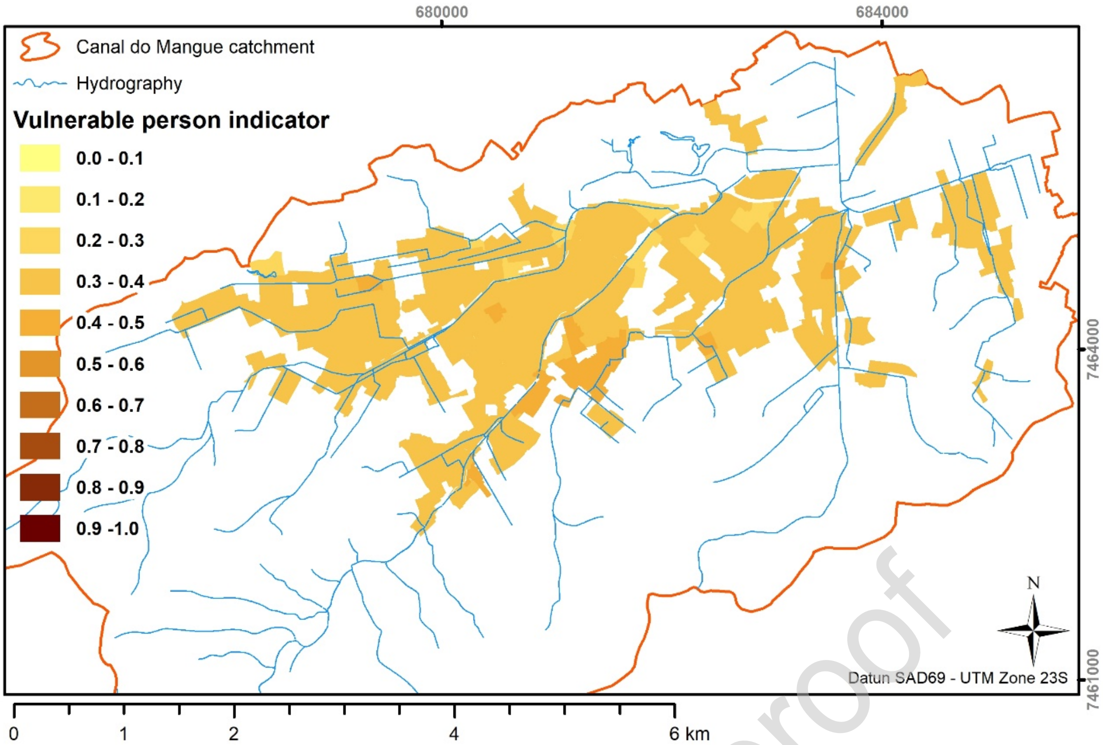

Figure 16. Mapping of the vulnerable people indicator (I_{VP}).

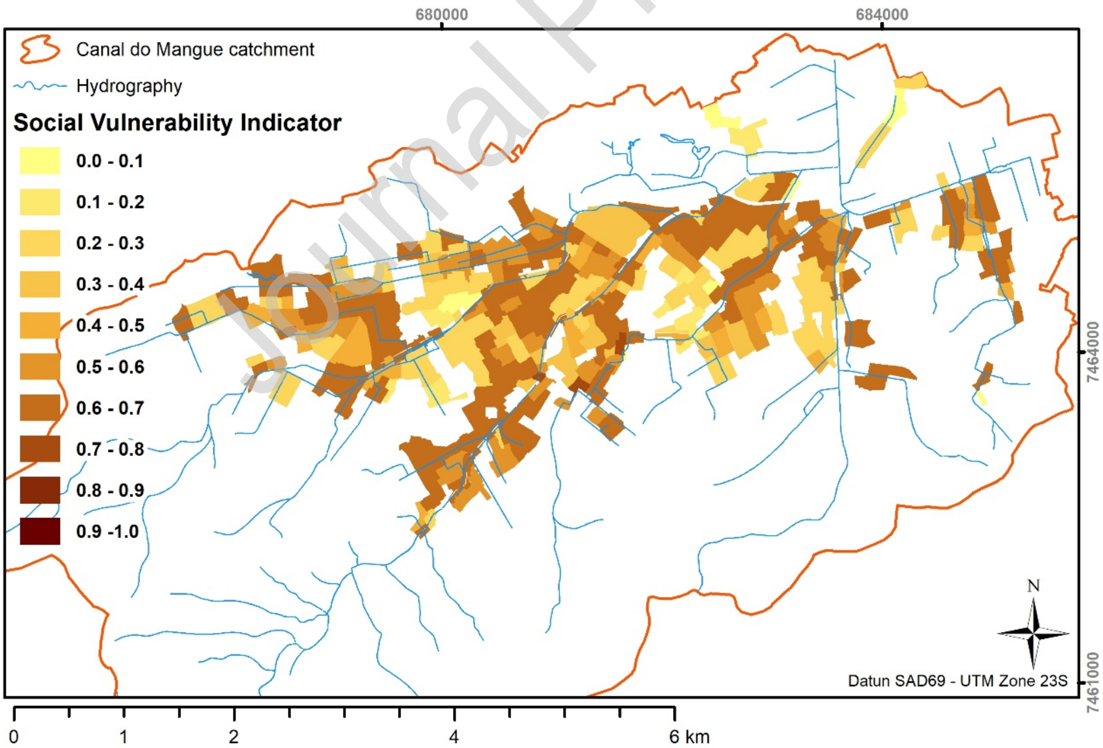

Figure 17. Mapping of the Social Vulnerability Indicator (I_{SV}).

Finally, the spatialized results in the Canal do Mangue basin of the Ri-SoRCI are presented in the map of Figure 18. The final composition of flood risk assessment, considering the Ri-SoRCI, does not point only to regions that concentrate more valuable properties, but it indicates the places that are more vulnerable to the damages and that could suffer more negative social impacts over time, because of the relative lower capacity to recover from flooding losses. The distribution of the higher risk zones in the Canal do Mangue catchment indicates a very critical situation, confirming the observed high frequent flooding problems in the region.

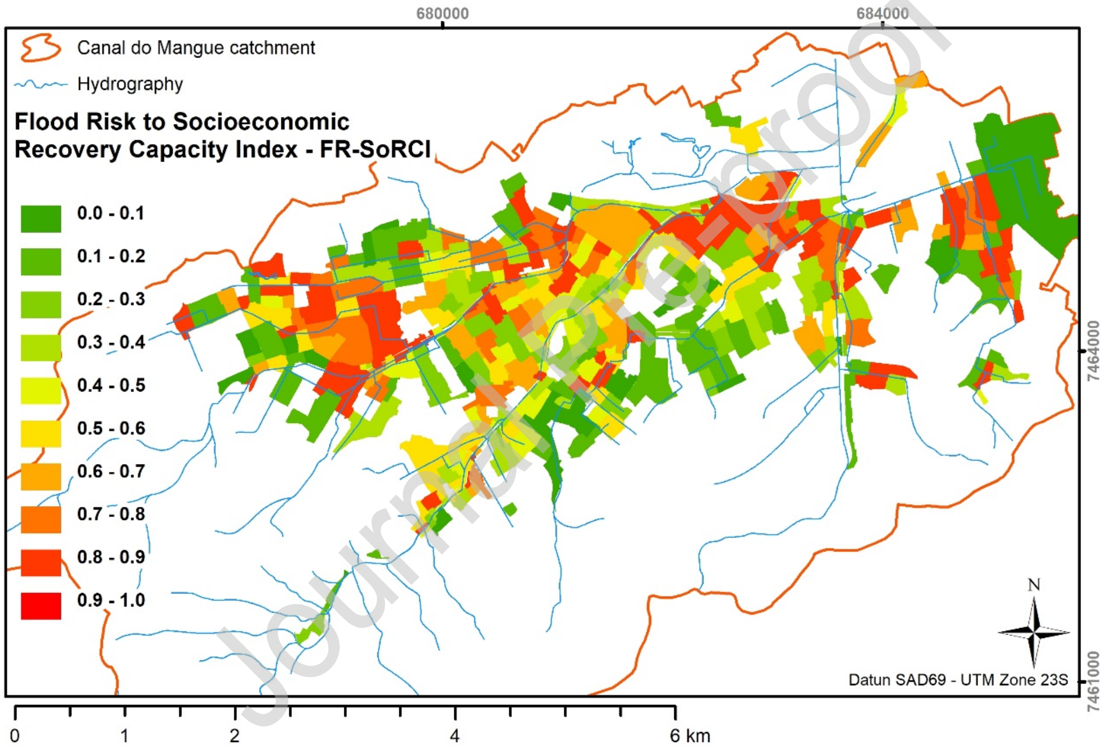

Figure 18. Mapping of the Risk to Socioeconomic Recovery Capacity Index (Ri-SoRCI).

This situation can be illustrated by comparing two regions inside the basin, that present different socioeconomic patterns but show similar flooding result. It was chosen a region localized along the Trapicheiros River (higher average income) and other localized in the Papa-Couve River (lower average income). The analysis of the result shows the potential of the Ri-SoRCI mapping in relativizing the flood losses among richer and poorer areas. The severity of the flood risk is higher when inhabitants have higher socioeconomic vulnerability, given a certain flooding depth. Figure 19 shows the process of analysis that allows this conclusion.

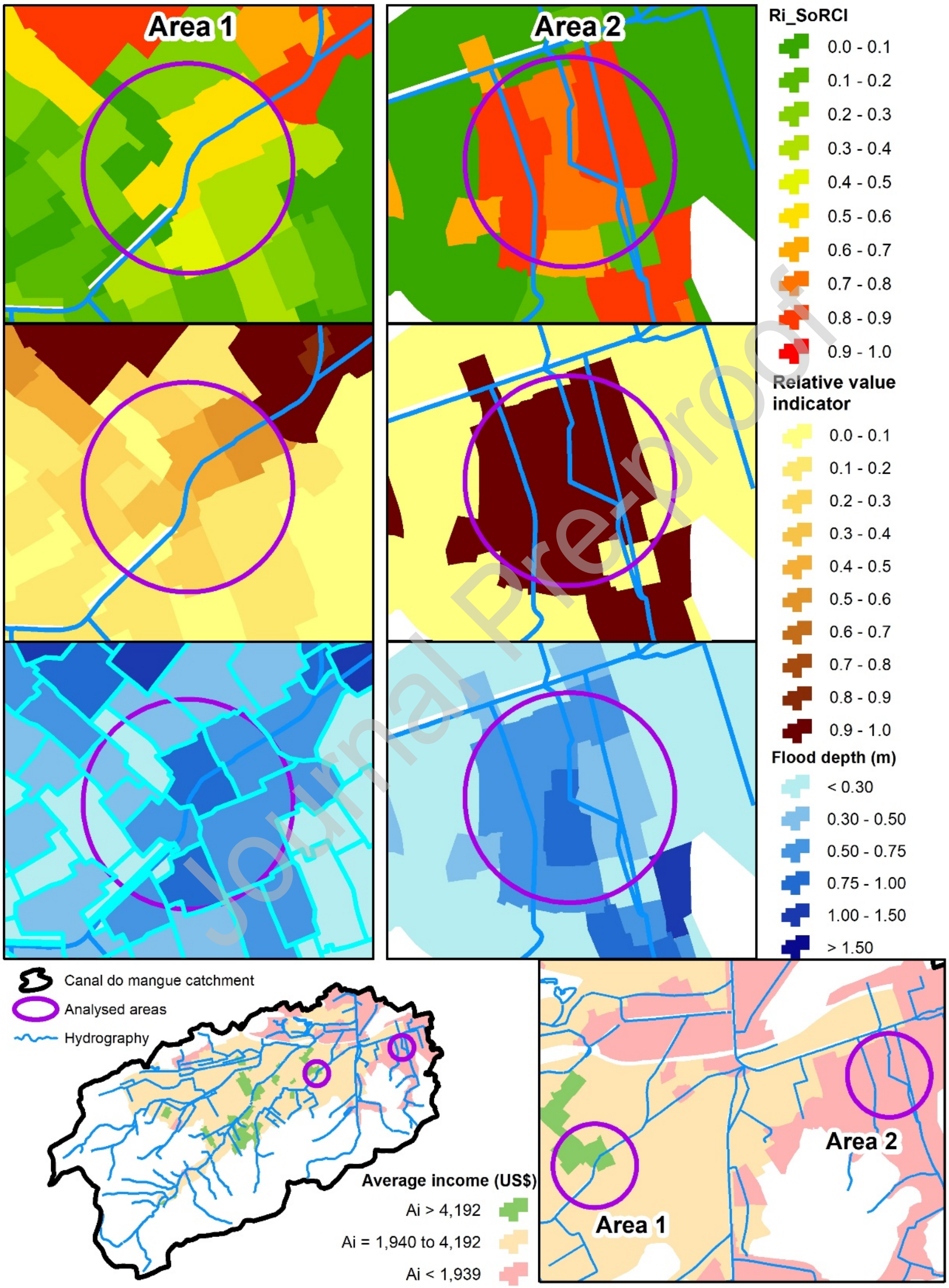

Figure 19. Flood risk comparison among two areas with different socioeconomic patterns and similar flooding depths. Area 1 is in the Trapicheiros River and area 2 is in the Papa-Couve River.

The final mapping shows a very critical situation, with 24% of the area of interest classified as high or very high risk zones (Ri-SoRCI > 0,60). This value was estimated considering risk ranges as shown in Table 6. The areas were classified and compared to the whole area of interest. This result can be seen in Figure 20.

Table 6. Flood risk classes

Flood Risk	Ri_SoRCI		
Very low	0.00	-	0.25
Low	0.25	-	0.49
Moderate	0.50	-	0.69
High	0.70	-	0.89
Very high	0.90	-	1.00

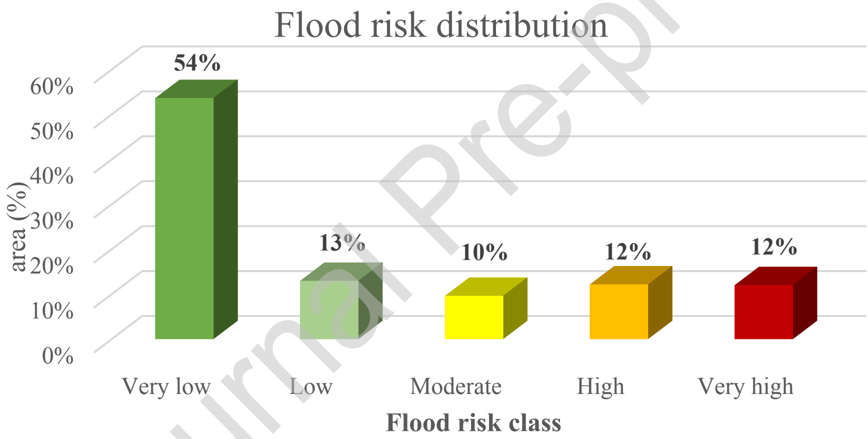

Figure 20. Flood risk distribution in the Canal do Mangue catchment, using the Ri_SoRCI.

6. CONCLUSION

Risk factors are associated with a certain degree of exposure to a critical natural or social situation that causes vulnerability in certain groups. In a more recent approach, researchers bring a temporal (future) perspective in the concept of vulnerability, establishing that the most vulnerable groups are also those that face the greatest difficulties to rebuild their lives after a disaster. Thus, these same groups may become more vulnerable to the effects of subsequent disasters.

Therefore, finding a way to measure vulnerability, considering the socioeconomic aspects, has become an important demand for a better management of flood risks. The Risk to Socioeconomic Recovery Capacity Index (Ri-SoRCI) aims to cover part of this demand. It brings into account not only a direct measure of flood damages, but also a relative perception of losses, that varies with socioeconomic classes.

When mapping the flood risks of a community using Ri-SoRCI, decision-making can be more sensitive to population groups exposed to floods that do not represent a significant part of the potential economic losses resulting from an event. The spatialization of the index turn it possible to better detail projects in order to enhance their outcomes, allowing prioritization of socially vulnerable regions. In other words, it enables the identification of sensitive areas that are in the greatest need of improvement.

The Ri-SoRCI could subside decision making process of public investments, helping stakeholders in choosing priority areas to receive interventions or what is the better set of interventions to reduce flood risk in a determined region. The public policies for territory and urban planning can consider the flood risk mapping to ordinate the land use and land cover. Future scenarios simulations can be done to support this ordination over time, forecasting potential impacts of unpredicted events.

Additionally, it should be noted that the main aim of this study was to propose a new index formulation. The weighting assessment was simplified here, although it is of great importance to the final results in practical application. While the weighting process can be part of the modeler decision, in agreement with stakeholders' choices to prioritize the risk parcels that are more sensible for each specific undergoing evaluation, a next step in this research should consider a sensitivity analysis to help in the weights definition process.

It is also important to stress that the index proposed in this paper is part of a resilience evaluation framework, developed to allow the internalization of residual risk in flood control design studies.

There are several potential improvements to be done, considering other social vulnerability indicators, as population education and health care system coverage, weighting assessment, among others.

ACKNOWLEDGEMENTS

The authors wish to acknowledge the financial support provided by the Coordenação de Aperfeiçoamento de Pessoal de Nível Superior- Brasil (CAPES) [Finance Code 001]; Conselho Nacional de Desenvolvimento Científico e Tecnológico (CNPq) [141065/2012-5] and the technical support provided by the Aquafluxus Water Resources Environmental Consulting.

REFERENCES

Andoh, R.Y.G., Iwugo, K.O., 2002. Sustainable Urban Drainage Systems: A UK Perspective, in: Global Solutions for Urban Drainage. American Society of Civil Engineers, Reston, VA, pp. 1–16. https://doi.org/10.1061/40644(2002)19

Balica, S.F., Douben, N., Wright, N.G., 2009. Flood vulnerability indices at varying spatial scales. Water Sci. Technol. 60, 2571–2580. https://doi.org/10.2166/wst.2009.183

Barbosa, A.E., Fernandes, J.N., David, L.M., 2012. Key issues for sustainable urban stormwater management. Water Res. 46, 6787–6798. https://doi.org/10.1016/j.watres.2012.05.029

Bradshaw, C.J.A., Sodhi, N.S., Peh, K.S.H., Brook, B.W., 2007. Global evidence that deforestation amplifies flood risk and severity in the developing world. Glob. Chang. Biol. 13, 2379–2395. https://doi.org/10.1111/j.1365-2486.2007.01446.x

Brown, R.R., Keath, N., Wong, T.H.F., 2009. Urban water management in cities: historical, current and future regimes. Water Sci. Technol. 59, 847–855. https://doi.org/10.2166/wst.2009.029

Chow, V. Te, 1959. Open-channel hydraulics. McGraw-Hill, New York.

Chow, V.., Maidment, D.R., Mays, L.W., 1988. Applied Hydrology, Internatio. ed. McGraw-

Hill, Singapore.

Chuah, C.J., Varis, O., Dąbrowski, M., Ziegler, A.D., Chan, F.K.S., 2018. Towards resilient flood risk management for Asian coastal cities: Lessons learned from Hong Kong and Singapore. J. Clean. Prod. 187, 576–589. https://doi.org/10.1016/j.jclepro.2018.03.217

COPPETEC, 2000. Execução de concepção e de projetos de obras civis e ações de controle das enchentes na Bacia Hidrográfica do Canal do Mangue. Rio de Janeiro.

De Roo, A., Schmuck, G., Perdigao, V., Thielen, J., 2003. The influence of historic land use changes and future planned land use scenarios on floods in the Oder catchment. Phys. Chem. Earth 28, 1291–1300. https://doi.org/10.1016/j.pce.2003.09.005

DESA/UN-WUP, 2018. World Urbanization Prospects: The 2018 Revision. Dep. Econ. Soc. Aff. 2.

Dutta, D., Herath, S., Musiake, K., 2003. A mathematical model for flood loss estimation. J. Hydrol. 277, 24–49. https://doi.org/10.1016/S0022-1694(03)00084-2

European Union, 2007. The European Floods Directive 2007/60/EC on the assessment and management of flood risks. Off. J. Eur. Union 288, 27–34. https://doi.org/English

Gallopín, G.C., 2006. Linkages between vulnerability, resilience, and adaptive capacity. Glob. Environ. Chang. 16, 293–303. https://doi.org/10.1016/j.gloenvcha.2006.02.004

Godschalk, D.R., 2003. Urban Hazard Mitigation: Creating Resilient Cities. Nat. Hazards Rev. 4, 136–143. https://doi.org/10.1061/(asce)1527-6988(2003)4:3(136)

Gogate, N.G., Kalbar, P.P., Raval, P.M., 2017. Assessment of stormwater management options in urban contexts using Multiple Attribute Decision-Making. J. Clean. Prod. 142, 2046–2059. https://doi.org/10.1016/j.jclepro.2016.11.079

Goonetilleke, A., Thomas, E., Ginn, S., Gilbert, D., 2005. Understanding the role of land use in urban stormwater quality management. J. Environ. Manage. 74, 31–42. https://doi.org/10.1016/j.jenvman.2004.08.006

Hoegh-Guldberg, O., Jacob, D., Taylor, M., 2018. Special Report on Global Warming of 1.5 °C - Chapter 3: Impacts of 1.5º C global warming on natural and human systems 243. https://doi.org/10.1002/ejoc.201200111

IBGE, 2004. 2002-2003 Household Budget Survey: First Results: Brazil and Major Regions. Rio de Janeiro, Brazil.

Jha, A.K., Bloch, R.B., Lamond, J., 2012. Cities and Flooding: A Guide to Integrated Urban Flood Risk Management for the 21st Century, Journal of Regional Science. https://doi.org/10.1111/jors.12006_6

Johannessen, Å., Wamsler, C., 2017. What does resilience mean for urban water services? Ecol. Soc. 22. https://doi.org/10.5751/ES-08870-220101

Kelman, Ii., 2003. Defining Risk. Risk Manag. 6–8. https://doi.org/10.4324/9780203359464_chapter_3

Kirby, A., 2005. SuDS - innovation or a tried and tested practice ? Proc. Inst. Civ. Eng. 1–8. https://doi.org/10.1680/muen.2005.158.2.115

Koks, E.E., Jongman, B., Husby, T.G., Botzen, W.J.W., 2015. Combining hazard, exposure and social vulnerability to provide lessons for flood risk management. Environ. Sci. Policy 47, 42–52. https://doi.org/10.1016/j.envsci.2014.10.013

Lavell, A., Mansilla, E., Smith, D., Brenes, A., Romano, L., Somarriba, H., Gamarra, L., Armien, F., 2003. La gestión local del riesgo - Nociones y precisiones en torno al concepto y la práctica. Guatemala.

Liao, K.-H., 2012. A Theory on Urban Resilience to Floods. Ecol. Soc. 17. https://doi.org/10.5751/ES-05231-170448

Lind, N., Hartford, D., Assaf, H., 2004. Hydrodynamic models of human stability in a flood. J. Am. Water Resour. Assoc. 40, 89–96. https://doi.org/10.1111/j.1752-1688.2004.tb01012.x

Machado, M.L., Nascimento, N., Baptista, M., Gonçalves, M., Silva, Adriano, Lima, J.C. De, Dias, R., Silva, Anderson, 2005. Curvas de danos de inundacao Versus Profundidade De Submersão : Desenvolvimento De Metodologia. Rega 2, 35–32.

Mahmoud, S.H., Gan, T.Y., 2018. Multi-criteria approach to develop flood susceptibility maps in arid regions of Middle East. J. Clean. Prod. 196, 216–229. https://doi.org/10.1016/j.jclepro.2018.06.047

Mascarenhas, F.C.B., Miguez, M.G., 2002. Urban flood control through a mathematical cell model. Water Int. 27, 208–218. https://doi.org/10.1080/02508060208686994

Meehl, G.A., Stocker, T.F., Collins, W.D., Friedlingstein, P., Gaye, A.T., Gregory, J.M., Kitoh, A., Knutti, R., Murphy, J.M., Noda, A., Raper, S.C.B., Watterson, I.G., Weaver, A.J., Zhao, Z.C., 2007. 2007: the Physical Science Basis. Cambridge Univ. Press. Cambridge, United Kingdom New York, NY, USA. Contrib. Work. Gr. I to Fourth Assess. Rep. Intergov. Panel Clim. Chang. https://doi.org/10.1080/07341510601092191

Meerow, S., Newell, J.P., Stults, M., 2016. Defining urban resilience: A review. Landsc. Urban Plan. 147, 38–49. https://doi.org/10.1016/j.landurbplan.2015.11.011

Mendoza-Tinoco, D., Guan, D., Zeng, Z., Xia, Y., Serrano, A., 2017. Flood footprint of the 2007 floods in the UK: The case of the Yorkshire and The Humber region. J. Clean. Prod. 168, 655–667. https://doi.org/10.1016/j.jclepro.2017.09.016

Miguez, M.G., Battemarco, B.P., De Sousa, M.M., Rezende, O.M., Verόl, A.P., Gusmaroli, G., 2017. Urban flood simulation using MODCEL-an alternative quasi-2D conceptual model. Water (Switzerland) 9. https://doi.org/10.3390/w9060445

Nordman, E.E., Isely, E., Isely, P., Denning, R., 2018. Benefit-cost analysis of stormwater green infrastructure practices for Grand Rapids, Michigan, USA. J. Clean. Prod. 200, 501–510. https://doi.org/10.1016/j.jclepro.2018.07.152

Nur, I., Shrestha, K.K., 2017. An Integrative Perspective on Community Vulnerability to

Flooding in Cities of Developing Countries. Procedia Eng. 198, 958–967. https://doi.org/10.1016/j.proeng.2017.07.141

Penning-Rowsell, E.C., Chaterton, J.B., 1980. Assessing the benefits of flood alleviation and land drainage schemes, in: Proceedings of the Institution of Civil Engineers. Middlesex Polytechnic. Severn Trent Water Authority, pp. 295–315.

Petit-Boix, A., Sevigné-Itoiz, E., Rojas-Gutierrez, L.A., Barbassa, A.P., Josa, A., Rieradevall, J., Gabarrell, X., 2017. Floods and consequential life cycle assessment: Integrating flood damage into the environmental assessment of stormwater Best Management Practices. J. Clean. Prod. 162, 601–608. https://doi.org/10.1016/j.jclepro.2017.06.047

Reiter, P., 2000. INTERNATIONAL SEMINAR ON THE RESCDAM PROJECT International methods of risk analysis , damage evaluation and social impact studies concerning dam-break accidents 1–17.

Rezende, O.M., 2018. Quantitative analysis of flood resilience for urban planning: case of the canal do Mangue in-Rio de Janeiro. Universidade Federal do Rio de Janeiro.

Rio-Águas, 2010. Estudos Hidrológicos E Dimensionamento. Rio de Janeiro.

Saito, N., 2014. Challenges for adapting Bangkok's flood management systems to climate change. Urban Clim. 9, 89–100. https://doi.org/10.1016/J.UCLIM.2014.07.006

Salgado, J.C.M., 1995. Economic Assessment of Drainage and Flood Control Projects in Urban Basins. Universidade Federal do Rio de Janeiro.

Sayers, P., Yuanyuan, L., Galloway, G., Penning-Rowsell, E., Fuxin, S., Kang, W., Yiwei, C., Le Quesne, T., 2013. Flood Risk Management A Strategic Approach Part of a series on strategic water management Flood Risk Management A Strategic Approach. Paris, France.

Sayers, P.B., Hall, J.W., Meadowcroft, I.C., 2002. Towards risk-based flood hazard management in the UK. Proc. Inst. Civ. Eng. - Civ. Eng. 150, 36–42. https://doi.org/10.1680/cien.2002.150.5.36

Shivaprasad Sharma, S. V., Roy, P.S., Chakravarthi, V., Srinivasa Rao, G., 2018. Flood risk assessment using multi-criteria analysis: A case study from Kopili river basin, Assam, India. Geomatics, Nat. Hazards Risk 9, 79–93. https://doi.org/10.1080/19475705.2017.1408705

Silva, B.M.G., Sousa, M.M. De, Rezende, O.M., Pitzer, A.C.J., De França, L.B.R., Miguez, M.G., Arrais, C.M., 2017. Use of multilevel model for urban flood evaluation, in: XXII Simpósio Brasileiro de Recursos Hídricos. ABRHidro, Florianópolis, pp. 1–8.

Silva, G.C.O., 2017. USO DE INSTRUMENTOS DA GESTÃO DO RISCO DE CHEIAS COMO FERRAMENTA NO PLANEJAMENTO URBANO. COPPE-UFRJ. UFRJ.

Tingsanchali, T., 2012. Urban flood disaster management. Procedia Eng. 32, 25–37. https://doi.org/10.1016/j.proeng.2012.01.1233

UNESCO, 2013. Flood Risk Management: A Strategic Approach, Water and Sewerage Journal. https://doi.org/10.1016/j.jacc.2006.07.056

US Department of the Interior, B. of R., 1987. Design of Small Dams, 3th ed. US Government Printing Office, Denver.

Vanneuville, W., Kellens, W., De Mayer, P., Reniers, G., Witlox, F., 2011. Is Flood Risk Management identical to Flood Disaster Management ? Earthzine 1–9.

Wouter Botzen, W.J., Bouwer, L.M., Scussolini, P., Kuik, O., Haasnoot, M., Lawrence, J., Aerts, J.C.J.H., 2019. Integrated Disaster Risk Management and Adaptation, in: Loss and Damage from Climate Change. Springer International Publishing, pp. 287–315. https://doi.org/10.1007/978-3-319-72026-5_12

WWAP/UN-Water, 2018. The United Nations World Water Development Report 2018: Nature-Based Solutions for Water. Paris, UNESCO.

Xiao, Y., Yi, S., Tang, Z., 2018. A Spatially Explicit Multi-Criteria Analysis Method on Solving Spatial Heterogeneity Problems for Flood Hazard Assessment. Water Resour. Manag. 32, 3317–3335. https://doi.org/10.1007/s11269-018-1993-6

Zanobetti, D., Lorgeré, H., 1968. Le modèle mathématique du Delta du Mékong. La Houille Blanche 17–30. https://doi.org/10.1051/lhb/1968002

Zeleňáková, M., Fijko, R., Labant, S., Weiss, E., Markovič, G., Weiss, R., 2019. Flood risk modelling of the Slatvinec stream in Kružlov village, Slovakia. J. Clean. Prod. 212, 109–118. https://doi.org/10.1016/j.jclepro.2018.12.008

Zevenbergen, C., Veerbeek, W., Gersonius, B., Van Herk, S., 2008. Challenges in urban flood management: travelling across spatial and temporal scales. J. Flood Risk Manag. 1, 81–88. https://doi.org/10.1111/j.1753-318x.2008.00010.x

CBIC - *Câmara Brasileira da Indústria da Construção*, 2019. Basic Unit Cost (Custo Unitário Básico). http://www.cub.org.br/ (accessed 1 October 2019).

IPP, 2019. Municipal Institute of Urbanization Pereira Passos, http://www.rio.rj.gov.br/web/ipp (accessed 1 October 2019).